

Magnetic Bias System for the Second Harmonic Cavity of the FNAL Booster

I. Terechkin

Addition of a tunable second harmonic accelerating cavity to the accelerating system of the FNAL Booster promises reduction of the beam loss during injection and transition periods [1]. The change of the resonant frequency from 75.732 MHz at the injection to 105.634 MHz at extraction must closely follow the accelerating cycle with 33.3 ms acceleration time and 15 Hz repetition rate; it is achieved by using a tuner that employs magnetically biased gyromagnetic material (AL800 garnet). As presently envisioned, the magnetic bias system includes a solenoid-type winding and a flux return that closes the magnetic circuit of the magnet and reduces fringe magnetic field. Two poles of the flux return concentrate the magnetic field in the region of the tuner. To avoid negative impact of the eddy currents in the flux return during magnetic field ramping, it must be assembled using profiles cut of thin sheets of silicon steel. Employing #24 (0.025" thick sheet) M15 or M19 silicon steel ensures sufficient dumping of the eddy currents.

Fig. 1 shows schematics of the bias magnet of the tuner used in the initial stage of design employing axially symmetric approach.

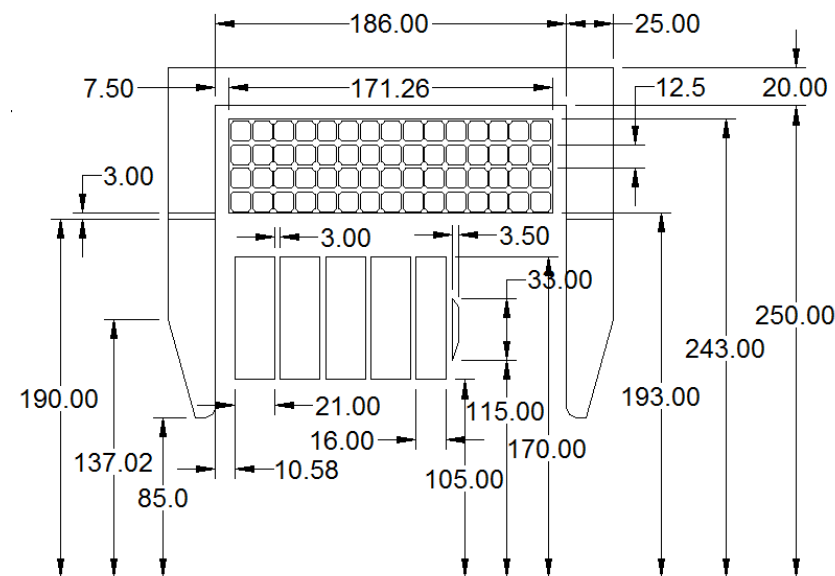


Fig. 1. Axially symmetric design concept of the magnetic system of the tuner.

The coil is wound using standard 0.41" square copper wire with $\varnothing 0.229$ " hole for cooling water (MA-186587). This wire is available in 90 feet reels. Geometrically, 60 turns can fit in the window of the flux return in Fig. 1, but a portion of the longitudinal space will be occupied by the leads, which will be taken out of the yoke radially. Cooling piping of the RF part of the tuner, which removes ~ 2 kW of the average power deposited in the gyrotropic material (see [2] for details), must also be taken out radially through the space occupied by the coil and openings in the flux return. Taking into account these restrictions, assuming just 50 turns in the bias coil looks like a reasonable starting point for the design.

Because of using laminated flux return and poles of the bias magnet and the gaps in the flux return for the cooling water piping, 3D modeling must be used to finalize the design.

The three-millimeter radial gap between the poles and the flux return in Fig. 1 was introduced as a temporary “convenience” feature that adds some flexibility to the flux return design. The size and the shape of this gap can be adjusted later to improve (or simplify) the magnetic and mechanical designs.

In this note, we assume the poles of the flux return assembled using laminated blocks made of profiles cut of silicon steel sheets. To reduce non-uniformity of the magnetic field in the tuner, gap between the blocks must be made as small as possible. The first approach to the pole design is shown in Fig. 2.

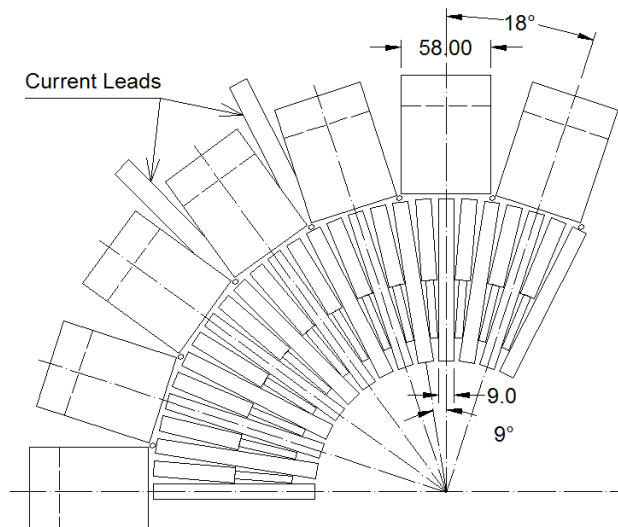


Fig. 2. Pole and the flux return of the bias magnet of the tuner.

This design was checked by direct modeling at the minimum bias current to make sure that the uniformity of the magnetic field in the garnet material is satisfactory and at the maximum current to verify the magnetic saturation state of the material in the poles and the flux return.

As a preliminary (quality control) step, some efforts were spent to make sure the results of 3D modeling follow the results made by a 2D study. During this step, the flux returns were made **axially symmetric** and identical for both 2D and 3D cases. Magnetic properties of the garnet material in the tuner are taken from [3], and magnetic modeling was made using COMSOL.

Graphs in Fig. 3 compare magnetic field calculated by 2D and 3D modeling along the radial lines inside the two end garnet blocks (left and right in Fig. 1) at $I_w = 6.65$ kA. The field distribution is almost identical for the 2D and 3D cases.

Beside this positive conclusion, this exercise provided an important hint that the shape of the flux return can make significant impact on the details of the distribution of the magnetic field in the gyrotropic material of the tuner. As a result, some re-optimization of the shim in the tuner will be required after the bias system design is finalized.

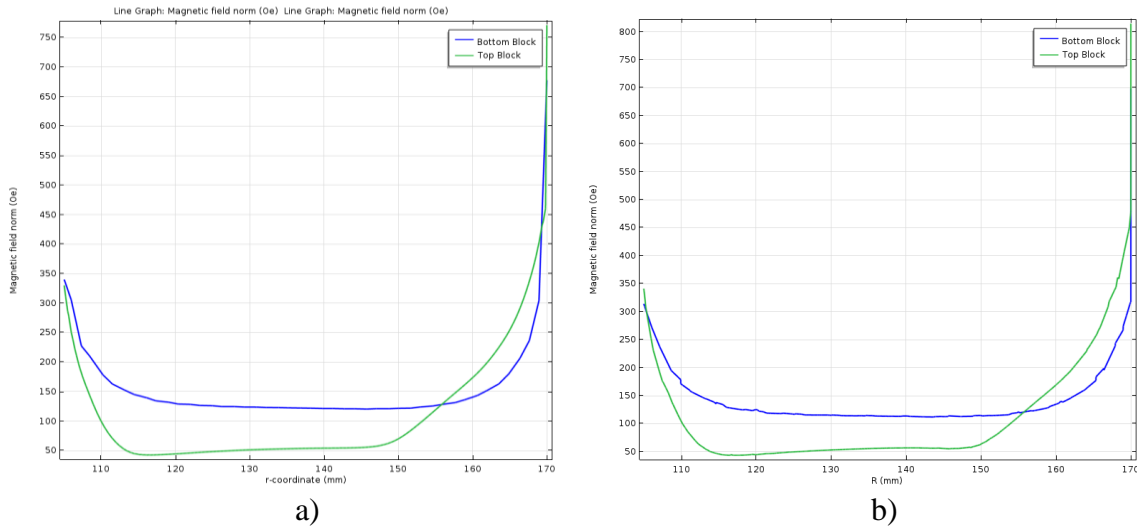


Fig. 3. Field distribution along the radial lines in the right garnet block (shown as “top block” in the figures) and the left garnet blocks (shown as “bottom block” in the figures) of the tuner obtained using 2D (a) and 3D (b) modeling. Axially symmetric case; $I_w = 6.65$ kA.

Sensitivity of the magnetic field distribution to the shape of the flux return manifests itself when the flux return and the poles lose their axial symmetry in the 3D model. Fig. 4 shows 3D model of the flux return with the pole design as in Fig. 2.

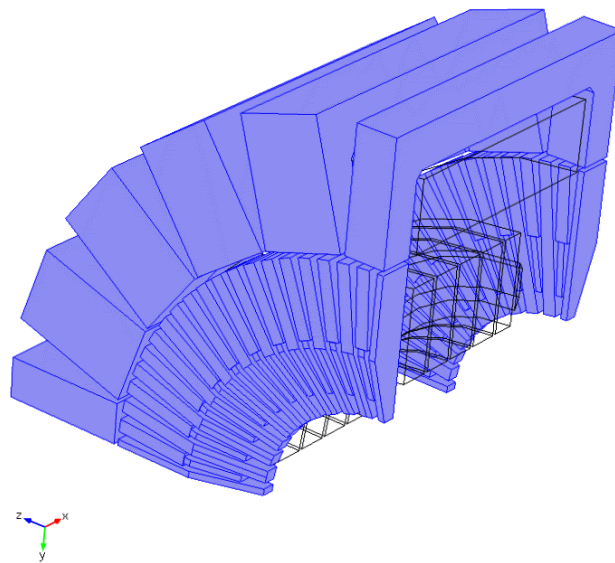


Fig. 4. Possible configuration of the flux return and the poles

As the poles and the flux return are not axially symmetric in this case, the field distribution is different along the sampling lines corresponding to different angular positions. It also differs from what the axially symmetric yoke configuration provides (Fig. 3).

Fig. 5 compares field distribution at the lowest bias current along the two sampling lines that are 4.5° apart. For the “bottom block” in the figure, the field is a bit higher when the sampling

goes through the longest pole piece is ($\phi = 0^\circ$). For the “top block”, as the distance to the pole is significant, the difference between the $\phi = 0^\circ$ and the $\phi = 45^\circ$ cases is negligible.

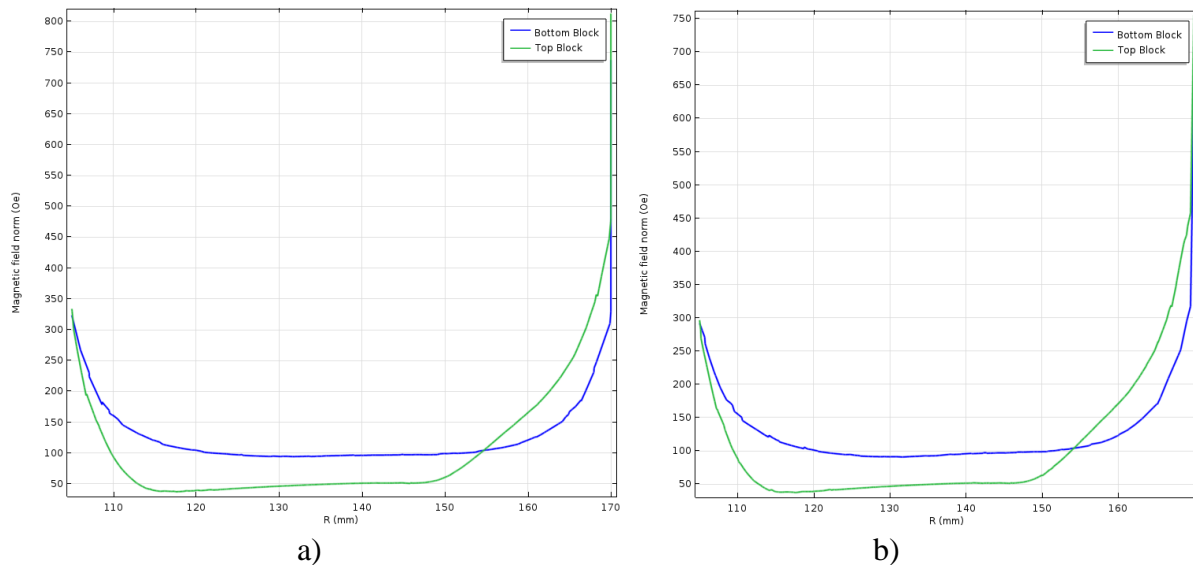


Fig. 5. Magnetic field along the sampling lines $\phi = 0$ (a) and $\phi = 4.5^\circ$ (b); $I_w = 6.65$ kA.

Although results of modeling are sensitive to the geometric shape of the flux return, they are not so sensitive to the shape of magnetization curves of the flux return material. If far from saturation, even constant permeability ($\mu = 5000$) approach provides results that compare well with the cases when non-linear properties are used. We will use saturation properties of M15 silicon steel shown in Fig. 6 in this study.

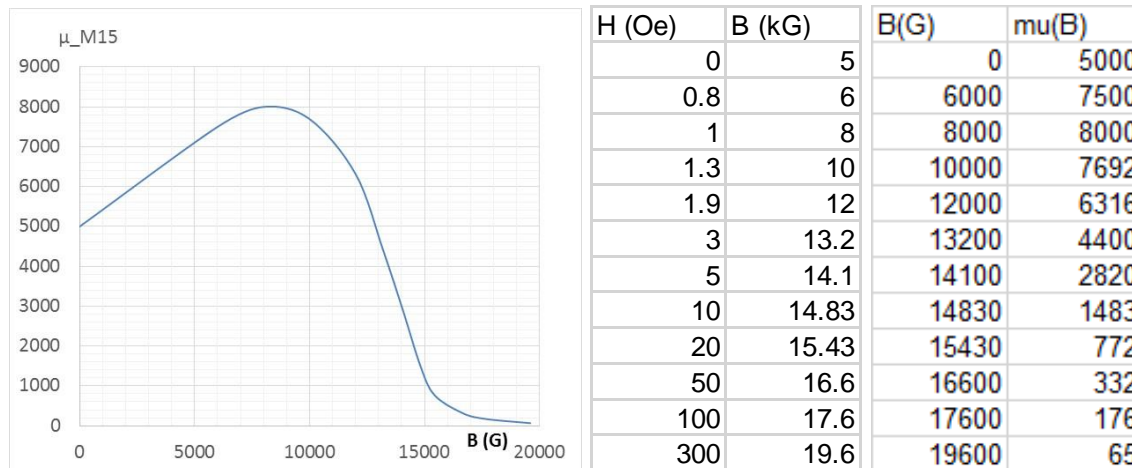


Fig. 6. M15 silicon steel magnetization curve

To make sure the poles and the flux return are not saturated at the maximum bias current of the tuner, we need to know the magnitude of this current first. Our experience of having several iterations of the RF design made shows that changes in the RF design often result in sensitive changes in the maximum bias current. As the RF design has not converged yet, in this note a case

will be used that required the highest magnitude of the maximum current. This case stems from the tuning curve presented on May 19, 2016 [4]. Fig. 7 shows the frequency ramp with two periods of the RF activities (a) and the tuning curve (b) of the cavity.

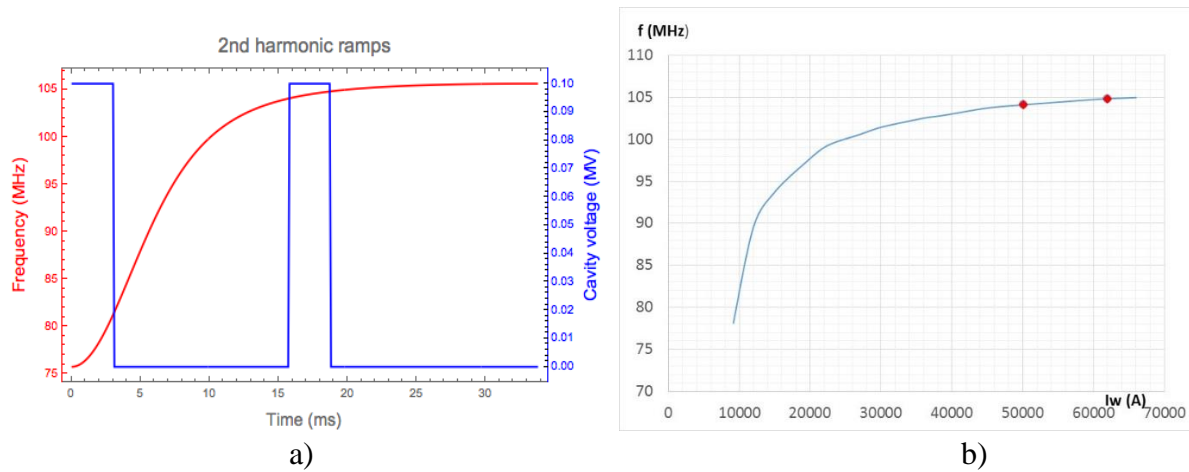


Fig. 7. Frequency ramp (a) and the tuning curve of the cavity (b).

Two markers on the tuning curve in Fig. 7-b show the bias current range that corresponds to the second active (transition) RF period ($16 \div 19$ ms). In this case, the maximum bias current is $I_w = 62.5$ kA. The change of the bias current in time that ensures the required frequency ramp can be found combining the two curves in Fig. 7. It is shown in Fig. 8a for the active part of the accelerating cycle from the injection to the end of the transition period: $0 \div 20$ ms. Having this curve along with the maximum current allows not only verification of the saturation state of the flux return at the maximum current, but also evaluation of the average power dissipated in the bias coil.

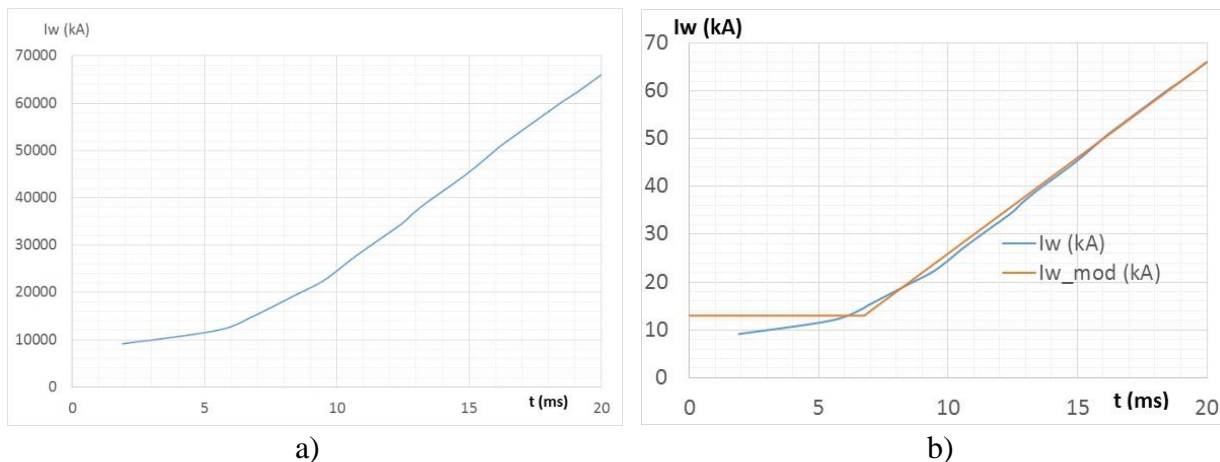


Fig. 8. Required bias current ramp during the active part of the accelerating cycle and its simplified approximation.

The average power in the coil was calculated using simplified shape of the bias current during active time period shown in Fig. 8b. The change of the bias current in time during the whole cycle can be described as the following:

$$I \cdot w = 13 \text{ kA when } t < 6.75 \text{ ms}$$

$$I \cdot w \text{ (kA)} = 13 + 4 \cdot (t[\text{ms}] - 6.75) \text{ when } 6.75 \text{ ms} < t < 20 \text{ ms}$$

$$d(I \cdot w)/dt = 4 \text{ kA/ms (dI/dt = 80 A/s if the number of turns } w = 50).$$

It is shown in Fig. 9. The maximum current at 20 ms is 1320 A. Starting at $t = 20$ ms, the current ramps down with the same ramp rate until it reached the initial value of 13 kA. Restricting the absolute value of the current ramp rate to the value needed during the acceleration period helps to limit the voltage of the power supply and the power dissipated in the coil. Other approaches, although possible, will result in higher dissipated power in the coil or the need of a higher voltage from the power supply during the down-ramp.

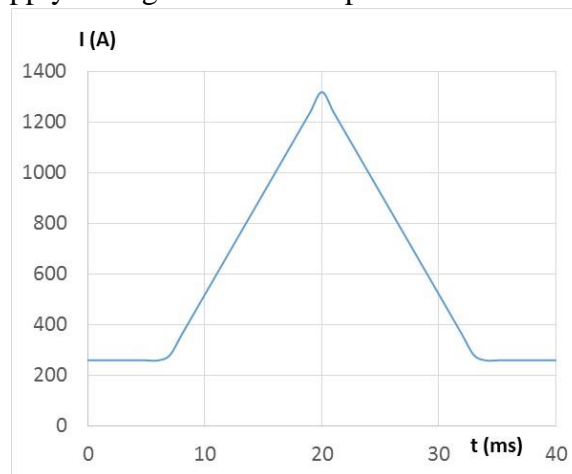


Fig. 9. Current ramp that is used to calculate the average power in the coil.

With some reserve, expected resistance of the 50-turn coil is 0.02 Ohm. Current as depicted by Fig. 9 generates 435 J of heat during one 66.6 ms long cycle. With 15 Hz repetition rate this results in ~6500 W of the average power deposited in the coil. This high power can be handled if four cooling circuits (one per each layer in Fig. 1) are used. In this case, assuming 1750 W of power and 10°C water temperature rise in the outer circuit, we get the required water flow in this circuit of 2.52 l/min, which translates in 1.6 m/s of the average velocity of water. With the 22 m length of this circuit, differential pressure of ~40 PSI is required in each cooling circuit.

The poles and the flux return shown in figures 1 and 2 experience significant saturation when the bias current approaches its maximum value of 1250 A ($Iw = 62.5 \text{ kA}$). The main reason of saturation is insufficient volume occupied by the steel in the flux return. This volume can be increased by increasing the thickness of the flux return and reshaping the plates of the poles. Fig. 10 shows improved profiles of the pole plates, and in Fig. 11 the modified geometry of the bias magnet is presented.

Compared with the geometry shown in figures 1 and 2, thickness of the flux return was increased to avoid saturation. To more evenly redistribute the magnetic flux in the plates of the poles, the gap between the poles and the flux return was reduced to 1 mm, and the inner surface of the opening in the flux return was made cylindrical.

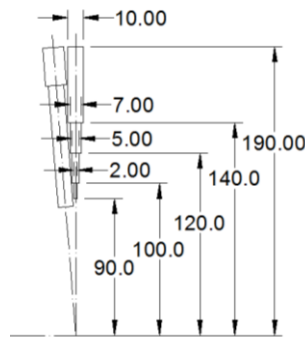


Fig. 10. Modified contours of the pole plates.

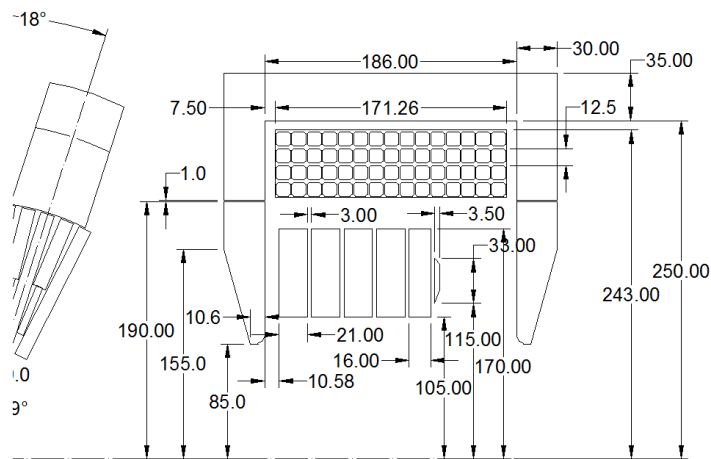


Fig. 11. Modified geometry of the bias system.

Fig. 12 shows the updated geometry of a 3D model used to calculate the magnetic field.

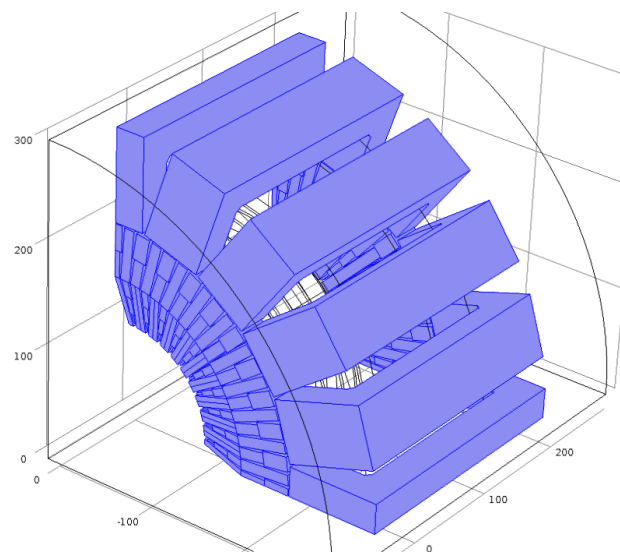


Fig. 12. Updated geometry of the COMSOL model

Fig. 13 shows the map of the flux density in the flux return at the maximum current in two planes: the inner surface of the pole and the 0° plane of longitudinal cross-section.

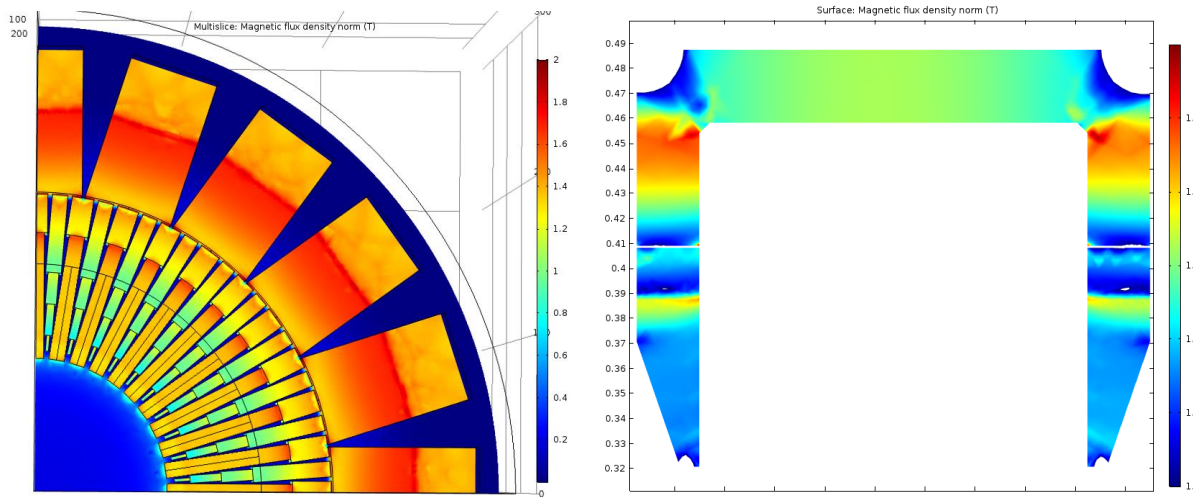


Fig. 13. Magnetic flux density in the flux return at 1250 A

Geometry modification resulted in significant improvement in the material saturation state. Further improvement can be achieved if to further increase the thickness of the pole pieces. This modification can be considered after the cavity assembly is finalized to free some additional longitudinal space.

With the improved saturation state, lower current is needed to reach the same permeability of the gyromagnetic material of the tuner. Fig. 14 shows the permeability and magnetic field in the garnet material at the 1250 A bias current with the modified magnetic circuit. The average permeability in the material became significantly lower than that required for the tuning to the maximum frequency at the transition (104.86 MHz).

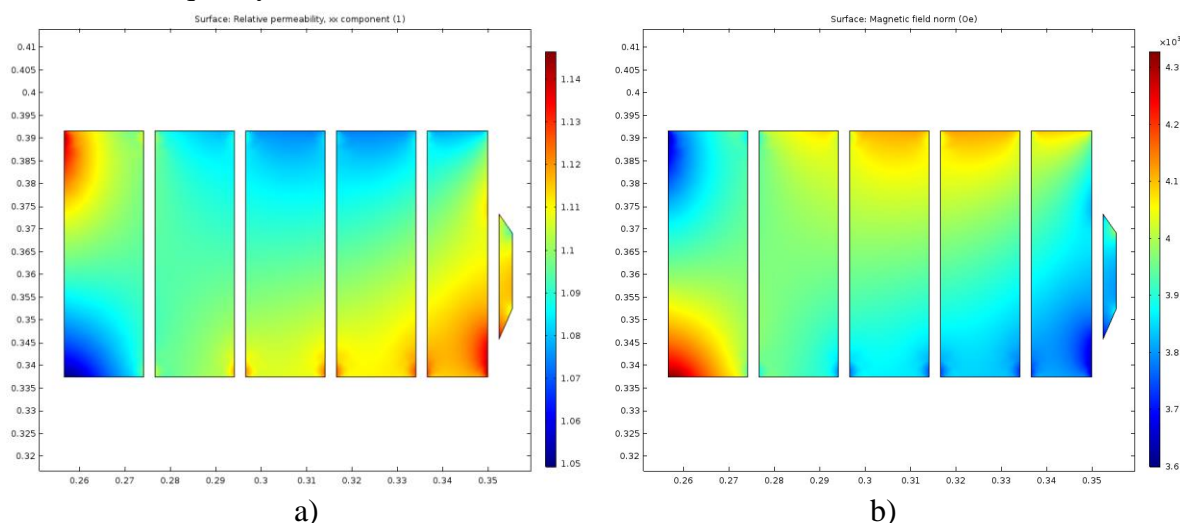


Fig. 14. Permeability (a) and magnetic field in Oersted (b) in the tuner of the cavity at the maximum current.

Although a welcomed improvement at high current, it can backfire at the low current if the magnetic field at the injection is too close to the gyromagnetic resonance condition.

The lowest frequency of 75.73 MHz corresponds to the total current $I_w = 7400$ A. This corresponds to the **148 A** current in the coil. Fig. 15 shows permeability and magnetic field in the garnet material at this current.

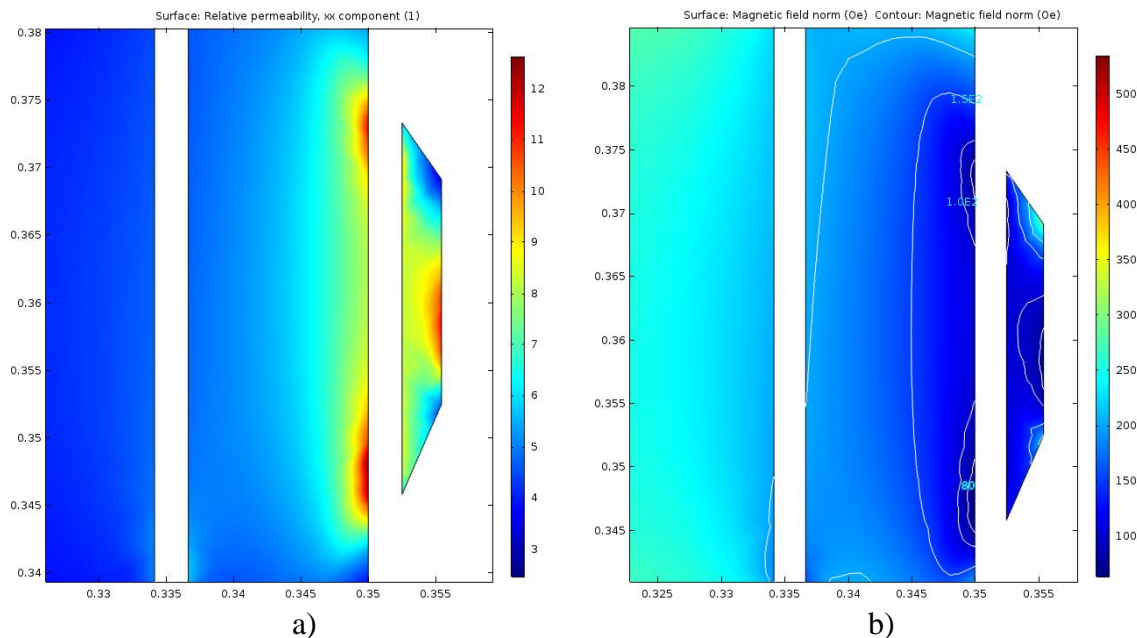


Fig. 15. Permeability (a) and magnetic field (b) in the garnet material at 148 A. Line contours correspond to the magnetic field levels of 80, 100, 150, and 200 Oe.

As the gyromagnetic resonance field at 75 MHz is ~ 32 Oe, we can conclude that we are still relatively far from the resonance.

Summary and Conclusion

Configuration of a bias magnetic system for the tuner of the second harmonic cavity of the Fermilab Booster is proposed. The system consists of a solenoid-type coil, and a flux return with two pole pieces. The flux return is assembled using profiles cut of gauge 24 sheets of M-15 silicon steel.

Study of this bias system configuration concluded that:

- The silicon steel material does not saturate at the maximum expected bias current.
- At the minimum current the magnetic field is still far from the gyromagnetic resonance condition.
- The heat generated in the coil can be removed by water circulating in the channel of the winding.

The concept design of the system must be finalized after the final version of the cavity is released. Mechanical design of the bias system can start as immediately after the concept design is approved.

References

1. G. Romanov, et al, “Perpendicular Biased Ferrite Tuned Cavities for the Fermilab Booster”, IPAC-2015, Richmond, VA, May 3-8, 2015.
2. I. Terechkine and G. Romanov, “Evaluation of Temperature Distribution in the Tuner of the FNAL Booster’s Tunable Second Harmonic Cavity”, FNAL TD note TD-16-002, February, 2016.
3. R. Madrak, et al, “Permeability of AL-800 Garnet Material”, FNAL TD note TD-15-014, June 2015
4. G. Romanov, “Mechanical Details of the CST Models” 2-nd harmonic cavity meeting, May 19, 2016, <http://beamdocs.fnal.gov/AD-public/DocDB/ShowDocument?docid=5158>